

Electron-Impact Ionization of Carbon

Nicolás Bachi ^{1,*} , Sebastian Otranto ^{1,*} and Karoly Tókési ^{2,*} 

¹ Instituto de Física del Sur (IFISUR), Departamento de Física, Universidad Nacional del Sur (UNS), CONICET, Av. L. N. Alem 1253, Bahía Blanca B8000CPB, Argentina

² Institute for Nuclear Research, 4026 Debrecen Bem tér 18/c, H-4026 Debrecen, Hungary

* Correspondence: nicolas.bachi@uns.edu.ar (N.B.); sotranto@uns.edu.ar (S.O.); tokesi@atomki.hu (K.T.)

Abstract: We present ionization cross-sections of collisions between electrons and carbon atoms using the classical trajectory Monte Carlo method. Total cross-sections are benchmarked against the reported experimental data and the predictions of numerically intensive theoretical methods as well as pioneering calculations for this collision system. At impact energies greater than about 100 eV, the present results are in very good agreement with the generalized oscillator strength formulation of the Born approximation as well as with the experimental data. Limitations inherent to a purely classical description of the electron impact ionization process at low impact energies are detected and analyzed, suggesting a clear route for future studies.

Keywords: electron impact; ionization of carbon; classical trajectory Monte Carlo

1. Introduction

The ITER project aims to demonstrate the feasibility of fusion as a large-scale energy source. It is currently under construction in Cadarache, France, and relies on the efforts of 35 countries to build the world's largest tokamak. Since the reactor has carbon components in its diverters, accurate data on the collision of electrons with carbon atoms are needed for plasma diagnostics, such as impurity influx studies [1].

Despite the potential interest in this topic, experimental reports on the ionization of C by electron impact are quite scarce. Total ionization cross-sections measured by Wang and Crawford are contained within an MIT internal report, which dates back to 1971, and were not published [2]. An accuracy of $\pm 30\%$ was estimated by the authors but practical details were not made explicit. A few years later, in 1978, Brook et al. published total cross-sections using the fast atom-beam and crossed electron-beam technique [3]. Their results, though consistent in shape, are lower than those of Wang and Crawford from the threshold up to an impact energy of 1 keV. No new data have been reported since then.

From a theoretical point of view, pioneering calculations by Peach, Omidvar et al. and McGuire made use of the Born–Ochkur approximation [4,5], the Born approximation [6], and a generalized oscillator strength formulation of the Born approximation [7], respectively. While the results of Peach (Refs. [4,5]) were consistent with the data of Wang and Crawford, the calculation of McGuire (Ref. [7]) supported the data of Brook et al. The results of Omidvar et al. (Ref. [6]) were right in between both datasets. During the last decade, efforts have been devoted to calculating the total ionization cross-section, either from the ground state or from excited states, by means of highly numerically intensive methods, such as the time-dependent close-coupling (TDCC), the time-independent distorted wave method (TIDW), the R-matrix-with-pseudostates (RMPS) and the B-spline R-matrix-with-pseudostates (BSR) [8,9]. These methods have provided results that are in fair agreement with the data of Brook et al. but were only extended up to 60 eV (TDCC, TIDW, RMPS) and 100 eV (BSR).

In the present work, we provide a complementary view of this collision system and calculate the total ionization cross-section for collisions of electrons with C by means of



Citation: Bachi, N.; Otranto, S.; Tókési, K. Electron-Impact Ionization of Carbon. *Atoms* **2023**, *11*, 16. <https://doi.org/10.3390/atoms11020016>

Academic Editor: Claudio Mendoza

Received: 15 December 2022

Revised: 14 January 2023

Accepted: 17 January 2023

Published: 20 January 2023



Copyright: © 2023 by the authors. Licensee MDPI, Basel, Switzerland. This article is an open access article distributed under the terms and conditions of the Creative Commons Attribution (CC BY) license (<https://creativecommons.org/licenses/by/4.0/>).

the three-body classical trajectory Monte Carlo (CTMC) method [10,11]. The CTMC is a non-perturbative method that, in contrast to highly numerically intensive methods, does not rely on huge basis sets, allowing its implementation in an ample impact energy range. Due to the large difference in the ionization potentials, the K-shell ionization cross-sections are negligible compared to those calculated for the outer shell. Therefore, the present calculations are restricted to the L-shell. Results obtained by means of the simple addition rule are contrasted to those provided by the independent electron model (IEL) and the independent event model (IEV). Limitations inherent to the classical treatment are identified and analyzed.

Atomic units are used throughout this work unless otherwise stated.

2. Theoretical Method

In this work, the three-body CTMC model in its microcanonical formulation is employed. Hamilton's equations are solved for the mutually interacting three-body system, in which the two electrons interact with each other via a Coulomb potential and with the ion core via the potential model derived from Hartree–Fock calculations by Green et al. [12] that was later on generalized by Garvey et al. [13],

$$V(r) = \frac{(N - 1)[1 - \Omega(r)] - Z}{r}, \tag{1}$$

$$\Omega(r) = \left[\left(\frac{\eta}{\zeta} \right) \left(e^{\zeta r} - 1 \right) + 1 \right]^{-1}. \tag{2}$$

This functional form allows the incorporation of the electronic screening effect, providing a more solid description of the collision dynamics compared to the use of fixed effective charges together with Coulomb potentials. Specific values for the parameters N , ζ , and η employed throughout the present study to represent the interaction of an electron with the C^+ and C^{2+} ions are shown in Table 1. The variation in the dynamical charge $Z(r) = -rV(r)$ with the electron-ion core distance is illustrated in Figure 1. As a general trend, the electron evolving in such model potential sees an asymptotic charge of +1 which gradually increases towards + Z as the electron-core distance tends to zero.

Table 1. Garvey model potential parameters for the C^+ and C^{2+} ions as provided in Ref. [13].

	C^+	C^{2+}
Z	6.0	6.0
N	6	5
ζ	1.065	1.5234
η	2.13	2.494

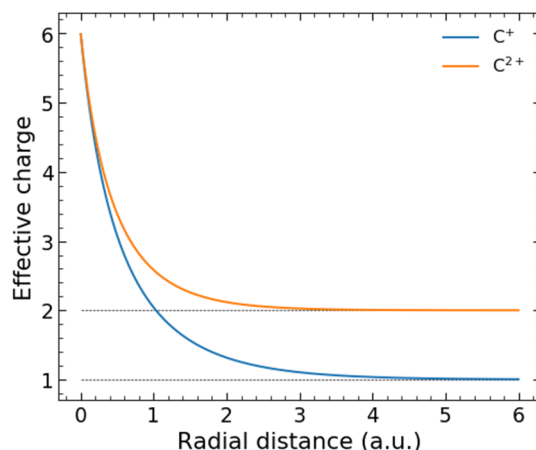


Figure 1. Garvey dynamical effective charge $rV(r)$ as a function of the radial distance for the C^+ and C^{2+} cores.

Collisional events are tracked until the momenta of all the particles are considered to be converged. The ionization probability as a function of the impact parameter b is determined by the ratio between the number of ionization events N_{ion} and the total number of evaluated trajectories N_{tot} .

$$P_{\text{ion}}(b) = \frac{N_{\text{ion}}(b)}{N_{\text{tot}}} \quad (3)$$

We use three different approaches to evaluate the total ionization probability as a function of the impact parameter:

(i) *Simple addition rule*

$$P_i(b) = 2(P_{\text{ion}, 2p}(b) + P_{\text{ion}, 2s}(b)) \quad (4)$$

where we add the ionization probabilities from the 2s and 2p orbitals.

(ii) *Independent electron model (IEL)*

$$P_{ii}(b) = 2P_{\text{ion}, 2p}(b)[1 - P_{\text{ion}, 2p}(b)][1 - P_{\text{ion}, 2s}(b)]^2 + 2P_{\text{ion}, 2s}(b)[1 - P_{\text{ion}, 2s}(b)][1 - P_{\text{ion}, 2p}(b)]^2 \quad (5)$$

where the multielectronic character of the target is considered by weighting the probability of electron emission from a given orbital by the probability of not removing additional electrons from the same or other orbitals of the neutral carbon atom. This model considers that the electron orbitals do not significantly change during the electron removal process.

(iii) *Independent event model (IEV)*

$$P_{iii}(b) = 2P_{\text{ion}, 2p}(b)[1 - P'_{\text{ion}, 2p}(b)][1 - P'_{\text{ion}, 2s}(b)]^2 + 2P_{\text{ion}, 2s}(b)[1 - P'_{\text{ion}, 2s}(b)][1 - P'_{\text{ion}, 2p}(b)]^2 \quad (6)$$

In this case, the probabilities P' in the weight factor represent probabilities of electron emission from the sequential C^+ ion.

Contributions from C(1s) are not explicitly considered in our work. We point out that explicit calculations for the ionization TCS from C(1s) at the punctual impact energies 500 eV, 750 eV, and 1000 eV were found negligible compared to the contributions of the 2s and 2p levels due to the large ionization potential of the C(1s) orbital.

The corresponding total ionization cross-section (TCS) is finally given by

$$\sigma_{k, \text{ion}} = 2\pi \int_0^{b_{\text{max}}} db b P_k(b), \quad (7)$$

with $k = (i), (ii), (iii)$. Here, b_{max} is the maximum impact parameter that can lead to ionization.

3. Results

In Figure 2 we show the TCS up to an impact electron energy of 1 keV and provide a quick view of our present state of knowledge. As indicated in the Introduction, it can be seen that early theoretical studies were far from conclusive regarding the discrepancy exhibited by the available experimental data. During the last decade, the implementation of numerically intensive techniques, such as TDCC, RMPS, and BSR lent credence to the dataset of Brook and the early theoretical prediction by McGuire. Regarding the present CTMC, results obtained by using the simple addition rule are in agreement with the experimental data and the theoretical results of McGuire at impact energies greater than about 100 eV. In contrast, the maxima of the TCS exhibit a clear shift towards lower impact energies compared to the data, and a clear overestimation of the threshold region is obtained. Similar trends have been reported in CTMC studies of electron impact ionization of hydrogen and helium [14].

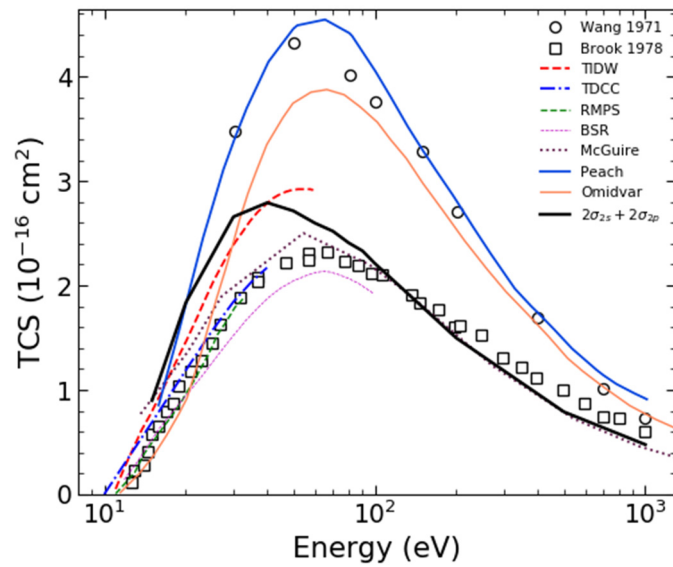


Figure 2. Total ionization cross-section as a function of the impact energy for collisions of electrons with carbon atoms. Expt: dots- Wang and Crawford (Ref. [2]), squares: Brook (Ref. [3]). Theories: dashed-red-line: TIDW, dotted-dashed-blue-line: TDCC, short-dashed-green-line: RMPS, all from Ref. [8]; short-dotted-pink line: BSR [9], solid-blue-line: Peach [4,5], solid-orange-line: Omidvar [6], dotted-magenta-line: McGuire [7], solid-black-line present CTMC results using the standard addition rule.

With the objective of determining whether this shift is provided by the consideration of separate contributions from the 2s and 2p orbitals, in Figure 3 we analyze the IEM and IEV description. We clearly observe that they do not lead to any improvement in this case, neither in terms of peak position or magnitude. These statements are confirmed in Figure 3b by a detailed inspection of $bP_k(b)$ as a function of b . We observe that the inclusion of the weight factors in Equations (6) and (7) leads to an energy-dependent global scaling factor but does not modify the shape of the distributions.

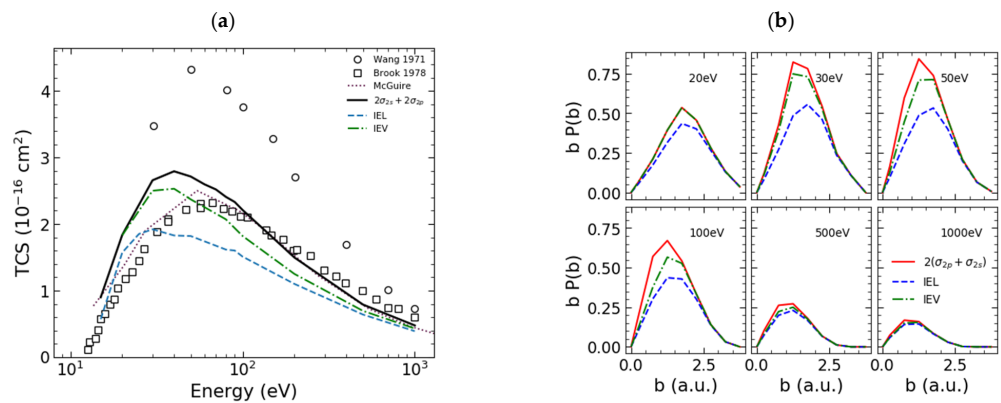


Figure 3. (a) Total ionization cross-section as a function of the impact energy for collisions of electrons with carbon atoms. Expt: dots- Wang and Crawford (Ref. [2]), squares: Brook (Ref. [3]). Theory: simple addition rule (filled line), IEL model (dash-dotted line), and IEV model (dashed line). (b) Ionization probability times impact parameter as a function of the impact parameter at different impact energies.

In order to gain insight into the limitations of the present classical procedure, we follow the line of reasoning developed by Kim and Rudd [15], Kim [16], and Kim and Desclaux [17] in their Binary-encounter-dipole model for electron-impact ionization and excitation of atomic targets.

It was shown that the total cross-sections produced by the plane-wave Born (PWB) approximation, a first-order theory that considers plane waves for the incoming and scattered projectile and approximate wave functions for non-hydrogenic targets, do not correctly describe the experimental data in the low energy range (impact energies lower than 100 eV) [15,16]. Such deficiency has been ascribed to the lack of electron exchange with the target electrons, the distortion of plane waves in the vicinity of the atomic target, or the polarization of the target due to the presence of the incident electron. To correct these deficiencies Kim and Rudd introduced a scaling method, called BEB-scaling [15]. In this scaling, the TCS for direct ionization of an electron in a bound orbital by an electron of incident energy T is given by

$$\sigma_{\text{BEB}} = \frac{4\pi a_0^2 N \left(\frac{R}{B}\right)^2}{t + u + 1} \left\{ \frac{\ln t}{2} \left(1 - \frac{1}{t^2}\right) + 1 - \frac{1}{t} - \frac{\ln t}{1+t} \right\}. \quad (8)$$

Here T and B are the impact energy and the ionization potential, respectively, R is the Ry constant, $t = T/B$, and $u = U/B$, and U is the orbital kinetic energy.

Similarly, a scaling for electron impact excitation, which was denominated BE and consists in multiplying the PWB total cross-section by an energy-dependent factor, was presented in Ref. [16]:

$$\sigma_{\text{BE}} = \sigma_{\text{PWB}} \frac{T}{T + B + E} \quad (9)$$

In this case, E is the excitation energy. In Ref. [17], Kim and Desclaux showed that these semiempirical scaling used together are able to reproduce Brook's data.

Following the spirit of those studies, we multiply our CTMC total ionization cross-sections by energy-dependent factors,

$$\sigma_{\text{ion}} = 2\sigma_{2p} \frac{T}{T + B_{2p}} + 2\sigma_{2s} \frac{T}{T + B_{2s}}. \quad (10)$$

This model, which we denominate B-CTMC, is not designed to provide the ultimate description of the data, but to help detect the limitations of our classical model instead. In this sense, for our purposes, we have explicitly omitted the E term in the denominator of the scaling factors. As can be seen in Figure 4, the agreement with the experimental data remarkably improves. While the B-CTMC results converge to the CTMC results at large impact energies, the peak position and the slope of the total cross-section near the threshold, are now in good agreement with the data. We have also added the recent scaled Distorted Wave Born Approximation (DWBA) results from Jonauskas (Ref. [18]), in which the receding projectile interaction with the target is either described by a potential that considers the neutral target, just as in the initial state or the already ionized target.

These results suggest that for the electron impact case, the CTMC is not providing an accurate description of the collision process at low impact energies. However, the possible issues indicated by Kim and Rudd for the PWB approximation do not seem to apply in this case. This is due to the fact that the CTMC model is a non-perturbative method, and explicitly considers the projectile interaction with the target electron and the ionic core throughout the whole collision process. In addition, electron exchange events take place and gain relevance for decreasing impact energies. To further illustrate this point, in Figure 5 we show some classical trajectories that lead to ionization and electron exchange for the 2p and 2s orbitals.

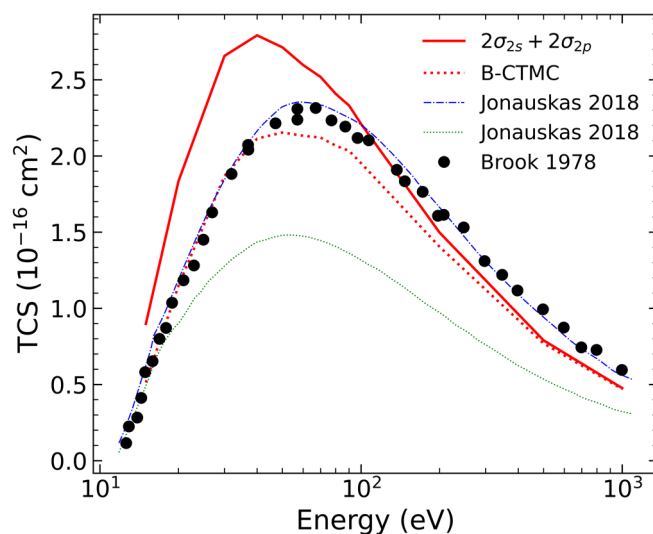


Figure 4. Ionization cross-section as a function of incident energy. Expt.: filled dots: Brook (Ref. [3]). Theories: dash-dotted-blue-line: DWBA in the potential of the ionizing ion (Ref. [18]), dotted-green-line: DWBA in the potential of the ionized ion (Ref. [18]), solid-red-line: present CTMC results using the standard addition rule, dotted-red-line: B-CTMC.

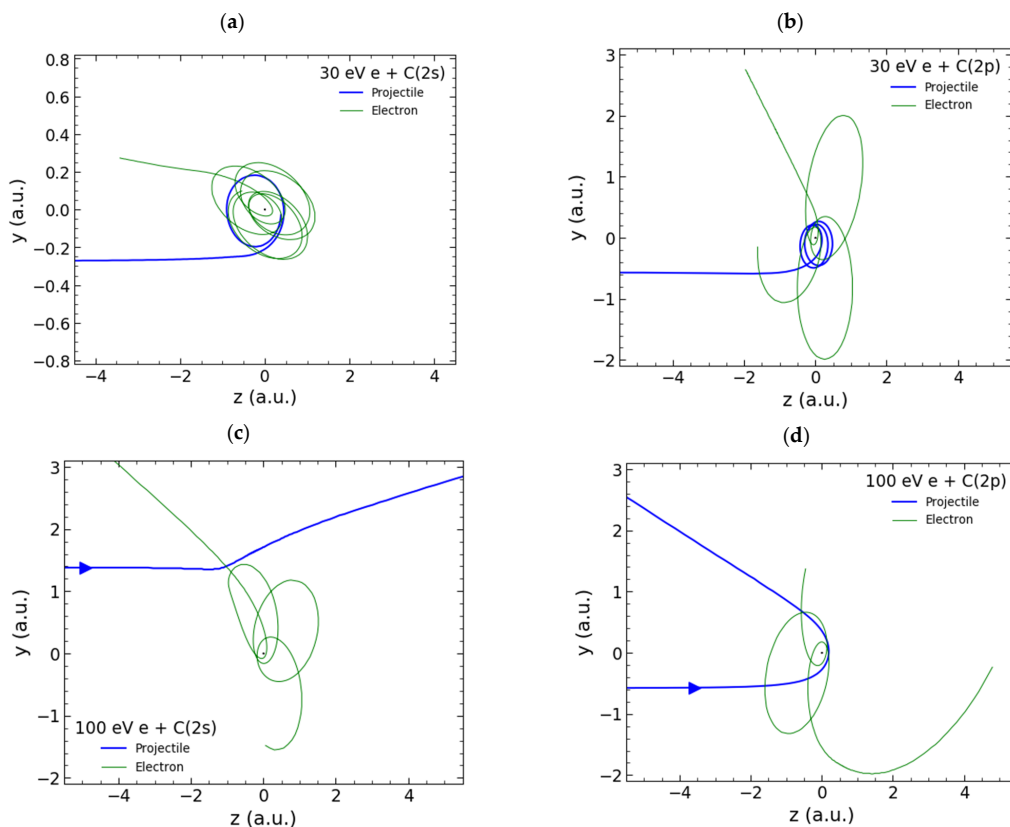


Figure 5. Classical trajectories in electron-carbon collisions. (a,b) correspond to exchange events between the projectile and 2s and 2p electrons, respectively. (c,d) correspond to ionization events and show trajectories of the projectile and electrons emitted from the 2s and 2p orbitals.

Two points are worth mentioning at this stage. On the one hand, the classical atom has no minimum energy for the ground state. This feature becomes especially relevant at low impact energies when the target electron can accommodate a more deeply bound state as the projectile approaches, leading to a transfer of kinetic energy to the projectile [14].

On the other hand, as the impact energy decreases the chance of having a transient negative ion increases. The negative ion of carbon has two bound states, the ground state $2s^2 2p^3 {}^4S^0$ and the excited state $2s^2 2p^3 {}^2D^0$ [19]. From the classical point of view, and in contrast to the prediction of quantum mechanics, atoms or ions with two or more bound electrons autoionize without the need for any external agent. Different alternatives have been proposed to avoid this spurious autoionization in target systems, like the Bohr atom [20], the neglect of the e-e interaction [21], the backward-forward propagation scheme [22], and the introduction of momentum-dependent stabilizing potential terms to the Hamiltonians [23–29]. In contrast, in this case, the duration of the transient C^- ion and the fraction of such events is expected to depend on the projectile electron energy. Therefore, it is hard to infer firsthand the role that the e-e interaction might have on the electron emission process. Hence, at this stage we inspect the transient lifetime of C^- ions, that is the lapse of time that the three-body system conforms to a C^- ion during collision events. In Figure 6 we show the obtained results for the 2p and 2s states at an impact energy of 30 eV, which reveal that these negative ions last for less than 1 a.u. of time.

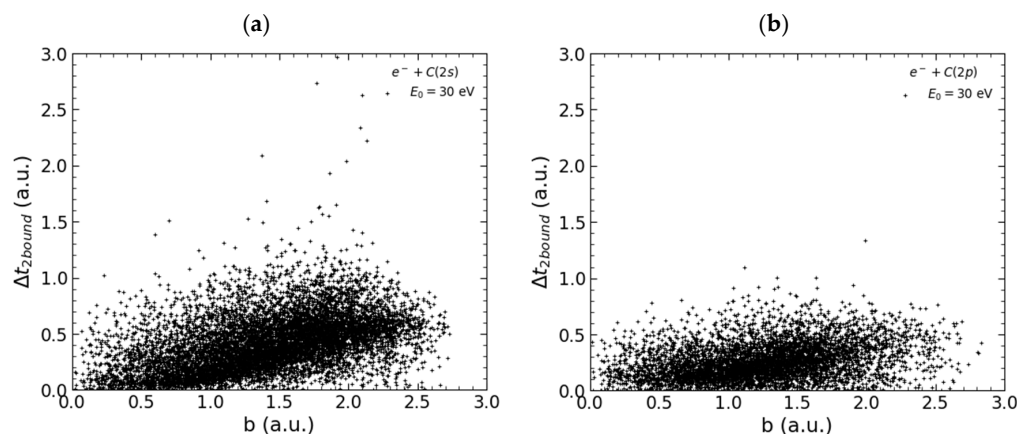


Figure 6. Classical transient lifetime of C^- ions registered in 30 eV electron-carbon collisions as a function of the impact parameter b , for (a) 2s and (b) 2p states.

Having determined the time scale, and with the aim of detecting whether or not this particular issue plays a role in the electron emission process, we decided to turn off the e-e interaction during the lapse that the two electrons were bound to the ionic core. In this drastic approach, the projectile and the target electron are only subjected to the field of the target nucleus during the transient lifetime of the C^- ion. The obtained results are shown in Figure 7. In Figure 7a we observe that the obtained total cross-section is now in much better agreement with the data, in terms of magnitude as well as peaking position. In addition, Figure 7b shows that the fraction of collision events in which transient C^- ions are found, increases with decreasing impact energy as expected. Moreover, the number of such events is found to be more relevant for the 2s orbital.

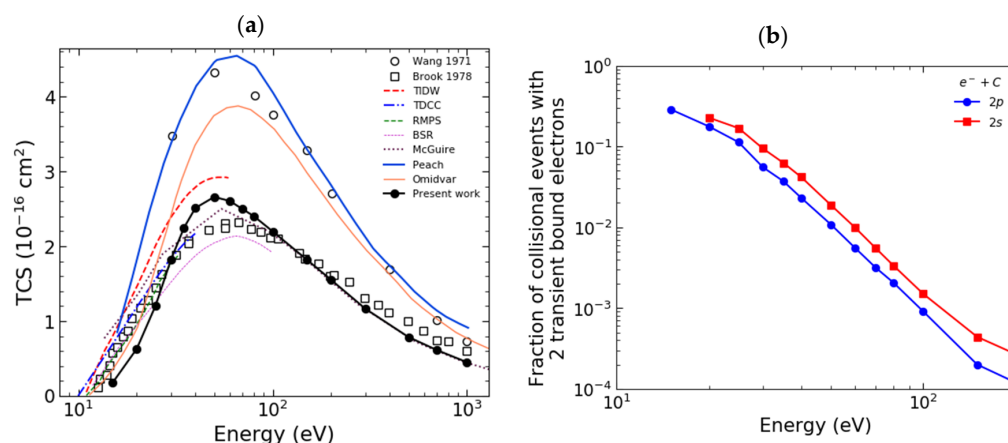


Figure 7. (a) Total ionization cross-section as a function of the impact energy for collisions of electrons with carbon atoms. Expt: dots- Wang and Crawford (Ref. [2]), squares: Brook (Ref. [3]). Present theory: simple addition rule in which the e-e is turned off during the transient C^- state. (b) Fraction of collisional events that conform to a transient C^- state as a function of the projectile electron impact energy. Line with blue circles: 2p state. Line with red squares: 2s state.

4. Discussion

Accurate data on electron carbon ionizing collisions are needed for diagnostic purposes in the power fusion reaction program. Although highly reliable numerically intensive methods have been used for this collision system during the past decade, these studies have been limited to impact energies lower than 100 eV. This highlights the need for reliable theoretical data at larger impact energies.

In this work, the classical description of the electron impact ionization of carbon has been analyzed as provided by the three-body CTMC method starting from the threshold region up to an impact energy of 1 keV.

Present results suggest that in its standard microcanonical formulation, and within the standard addition rule, the CTMC method is in perfect agreement with the results provided by the generalized oscillator strength formulation of the Born approximation of McGuire at impact energies greater than 100 eV and clearly support the data of Brook. In contrast, it tends to overestimate the electron emission at low impact energies. Furthermore, it predicts a clear shift of the peak of the total ionization cross-section towards lower impact energies.

A semi-empirical model following the spirit of those developed by Kim and Rudd clearly improved the agreement of the CTMC results with the data, suggesting that some physical aspects of the problem might not be accurately described by a classical description, especially at low impact energies.

Our inspection of the collision dynamics revealed the existence of transient C^- ionic states that the presently used Hamiltonian cannot properly describe. In order to test the potential relevance of these C^- ionic states in the electron emission process, the e-e interaction was turned off during their lapse of existence. This strategy led to a clear improvement in our CTMC predictions in the peak region of the TCS and opens a line of study that needs to be explored. Future studies should concentrate on the threshold region, usually denominated the Wannier region, where classical mechanics for the two-electron continuum is expected to apply and lead to a power law dependence of the TCS as a function of the impact energy [30].

Author Contributions: N.B. developed the CTMC code, performed numerical calculations, and contributed to the final manuscript. S.O. and K.T. developed CTMC codes, performed numerical calculations, contributed to the final manuscript and supervised the project. All authors have read and agreed to the published version of the manuscript.

Funding: This work has been carried out within the framework of the EURO fusion Consortium and has received funding from the Euratom research and training program 2014–2018 and 2019–2020 under grant agreement No 633053. The views and opinions expressed herein do not necessarily reflect those of the European Commission. The work was supported by the Bilateral relationships between Argentina and Hungary in science and technology (S&T) under project number 2019-2.1.11-TÉT-2020-00202. Work at IFISUR was supported by Grant No. PGI 24/F084, Secretaría General de Ciencia y Tecnología, Universidad Nacional del Sur.

Data Availability Statement: The data that support the findings of this study are available from the authors upon reasonable request.

Acknowledgments: The work was supported by the Bilateral relationships between Argentina and Hungary in science and technology (S&T) under project number 2019-2.1.11-TÉT-2020-00202. Work at IFISUR was supported by Grant No. PGI 24/F084, Secretaría General de Ciencia y Tecnología, Universidad Nacional del Sur.

Conflicts of Interest: The authors declare no conflict of interest.

References

1. Available online: www.iter.org (accessed on 15 December 2022).
2. Wang, K.I.; Crawford, C.K. *Electron Impact Ionization Cross Sections, Particle Optics Lab*; MIT Technical Report No 6, AFML-TR-70-289; MIT: Cambridge, MA, USA, 1971.
3. Brook, E.; Harrison, M.F.A.; Smith, A.C.H. Measurements of the electron impact ionisation cross sections of He, C, O and N atoms. *J. Phys. B At. Mol. Phys.* **1978**, *11*, 3115. [[CrossRef](#)]
4. Peach, G. Ionization of neutral atoms with outer 2p, 3s and 3p electrons by electron and proton impact. *J. Phys. B At. Mol. Phys.* **1970**, *3*, 328. [[CrossRef](#)]
5. Peach, G. Ionization of atoms and positive ions by electron and proton impact. *J. Phys. B At. Mol. Phys.* **1971**, *4*, 1670. [[CrossRef](#)]
6. Omidvar, K.; Kyle, H.L.; Sullivan, E.C. Ionization of multielectron atoms by fast charged particles. *Phys. Rev. A* **1972**, *5*, 1174. [[CrossRef](#)]
7. McGuire, E.J. Inelastic scattering of electrons and protons by the elements He to Na. *Phys. Rev. A* **1971**, *3*, 267. [[CrossRef](#)]
8. Abdel-Naby, S.A.; Ballance, C.P.; Lee, T.G.; Loch, S.D.; Pindzola, M.S. Electron-impact ionization of the C atom. *Phys. Rev. A* **2013**, *87*, 022708. [[CrossRef](#)]
9. Wang, Y.; Zatsarinny, O.; Bartschat, K. B-spline R-matrix-with-pseudostates calculations for electron-impact excitation and ionization of carbon. *Phys. Rev. A* **2013**, *87*, 012704. [[CrossRef](#)]
10. Abrines, R.; Percival, I.C. A generalized correspondence principle and proton-hydrogen collisions. *Proc. Phys. Soc.* **1966**, *88*, 873. [[CrossRef](#)]
11. Olson, R.E.; Salop, A. Charge-transfer and impact-ionization cross sections for fully and partially stripped positive ions colliding with atomic hydrogen. *Phys. Rev. A* **1977**, *16*, 531. [[CrossRef](#)]
12. Green, A.E.; Sellin, D.L.; Zachor, A.S. Analytic independent-particle model for atoms. *Phys. Rev.* **1969**, *184*, 1. [[CrossRef](#)]
13. Garvey, R.H.; Jackman, C.H.; Green, A.E.S. Independent-particle-model potentials for atoms and ions with $36 < Z \leq 54$ and a modified Thomas-Fermi atomic energy formula. *Phys. Rev. A* **1975**, *12*, 1144.
14. Schultz, D.R.; Meng, L.; Olson, R.E. Classical description and calculation of ionization in collisions of 100 eV electrons and positrons with He and H₂. *J. Phys. B At. Mol. Opt. Phys.* **1992**, *25*, 4601. [[CrossRef](#)]
15. Kim, Y.K.; Rudd, M.E. Binary-encounter-dipole model for electron-impact ionization. *Phys. Rev. A* **1994**, *50*, 3954. [[CrossRef](#)] [[PubMed](#)]
16. Kim, Y.K. Scaling of plane-wave Born cross sections for electron-impact excitation of neutral atoms. *Phys. Rev. A* **2001**, *64*, 032713. [[CrossRef](#)]
17. Kim, Y.K.; Desclaux, J.P. Ionization of carbon, nitrogen, and oxygen by electron impact. *Phys. Rev. A* **2002**, *66*, 012708. [[CrossRef](#)]
18. Jonauskas, V. Electron-impact double ionization of the carbon atom. *Astron. Astrophys.* **2018**, *620*, A188. [[CrossRef](#)]
19. Andersen, T.; Haugen, H.K.; Hotop, H. Binding energies in atomic negative ions: III. *J. Phys. Chem. Ref. Data* **1999**, *28*, 1511–1533. [[CrossRef](#)]
20. McKenzie, M.L.; Olson, R.E. Ionization and charge exchange in multiply-charged-ion–helium collisions at intermediate energies. *Phys. Rev. A* **1987**, *35*, 2863. [[CrossRef](#)]
21. Cohen, J.S. Formation of protonium in collisions of antiprotons with H and H[−]. *Phys. Rev. A* **1987**, *36*, 2024. [[CrossRef](#)]
22. Wetmore, A.E.; Olson, R.E. Electron loss from helium atoms by collisions with fully stripped ions. *Phys. Rev. A* **1988**, *38*, 5563. [[CrossRef](#)]

23. Geyer, T.; Rost, J.M. Dynamical stabilization of classical multi-electron targets against autoionization. *J. Phys. B At. Mol. Opt. Phys.* **2003**, *36*, L107. [[CrossRef](#)]
24. Geyer, T. Electron impact double ionization of helium from classical trajectory calculations. *J. Phys. B At. Mol. Opt. Phys.* **2004**, *37*, 1215. [[CrossRef](#)]
25. Kirschbaum, C.L.; Wilets, L. Classical many-body model for atomic collisions incorporating the Heisenberg and Pauli principles. *Phys. Rev. A* **1980**, *21*, 834. [[CrossRef](#)]
26. Zajfman, D.; Maor, D. “Heisenberg core” in classical-trajectory Monte Carlo calculations of ionization and charge exchange. *Phys. Rev. Lett.* **1986**, *56*, 320. [[CrossRef](#)] [[PubMed](#)]
27. Cohen, J.S. Quasiclassical-trajectory Monte Carlo methods for collisions with two-electron atoms. *Phys. Rev. A* **1996**, *54*, 573. [[CrossRef](#)] [[PubMed](#)]
28. Bachi, N.; Otranto, S. A closer insight into classical models for the He atom with two-active electrons. *Eur. Phys. J. D* **2018**, *72*, 1–8. [[CrossRef](#)]
29. Ziaeeian, I.; Tórkési, K. Interaction of Be⁴⁺ and ground state hydrogen atom—classical treatment of the collision. *Atoms* **2020**, *8*, 27. [[CrossRef](#)]
30. Wannier, G.H. The threshold law for single ionization of atoms or ions by electrons. *Phys. Rev.* **1953**, *90*, 817. [[CrossRef](#)]

Disclaimer/Publisher’s Note: The statements, opinions and data contained in all publications are solely those of the individual author(s) and contributor(s) and not of MDPI and/or the editor(s). MDPI and/or the editor(s) disclaim responsibility for any injury to people or property resulting from any ideas, methods, instructions or products referred to in the content.